

InP-BASED HBT WITH GRADED InGaAlAs BASE LAYER GROWN BY LP-MOVPE

S-O. Kim, P. Velling, M. Agethen, Th. Reimann, W. Prost, and F.-J. Tegude

*Department of Solid State Electronics, Gerhard-Mercator-University Duisburg,
Lotharstrasse 55 (ZHO), D-47057 Duisburg, Germany
Tel. 0203-379-3878, E-mail: kim@hlt.uni-duisburg.de*

ABSTRACT

A compositionally graded InGaAlAs:C base layer is inserted in an InP-based HBT grown by LP-MOVPE with a novel non-gaseous source configuration. Due to the addition of 6% Al the active hole concentration in the HBT base layer, deduced from Hall measurements, is increased from $1.5 \cdot 10^{19}$ to $3.8 \cdot 10^{19} \text{ cm}^{-3}$. Moreover, an In-grading within the base layer results in an intrinsic electric field of about 5.4 kV/cm. A high dc current gain of $\beta = 35$ is provided at a high p-type doping level. First HBT devices exhibit a current gain cut-off frequency of $f_T = 117 \text{ GHz}$ and an unilateral gain cut-off frequency of 90 GHz (not de-embedded).

INTRODUCTION

For high frequency performance of the Heterojunction Bipolar Transistor (HBT), it is desired to raise the p -doping level in the base layer in order to reduce contact and sheet resistance. Due to the low diffusivity carbon is preferred [1,2] as an alternative p -dopant over Zn and Be which both allow extreme high doping level but exhibit a comparatively high diffusivity [3,4] which can lead to degeneration of the device characteristics. However, the active hole concentration in carbon-doped InGaAs layer grown by MOVPE in device quality is limited to about $1\text{-}2 \cdot 10^{19} \text{ cm}^{-3}$ at 500 °C growth temperature [5]. A higher doping level could be achieved by lowering the growth temperature but material quality and electrical activity will be degraded [6]. Schneider et al. presented experimental results that the hole concentration can be significantly increased by adding Al in InGaAs layer [7]. The presence of Al enforces the incorporation of carbon on group-V lattice sites resulting in higher doping level. Recently, a device demonstration of an InGaAlAs base layer ($N_A = 1 \cdot 10^{19} \text{ cm}^{-3}$) in an HBT grown by MOVPE is reported [8]. Kurishima et al. have presented experimental results that HBTs with compositionally graded InGaAs base show a more than 50% improvement in current gain and about 20% in f_T compared to a uniform-base structure [9].

In this contribution we apply the approach of an InGaAlAs graded base in order to combine high p -type doping and a built-in field in the base. MOVPE growth is performed with non-gaseous source (ngs) configuration using nitrogen carrier gas and TBAs, TBP, and DitBuSi as replacement for the standard precursors AsH₃, PH₃, and Si₂H₆/SiH₄. The fabricated HBT using conventional optical lithography shows promising dc and rf characteristics.

EPITAXIAL GROWTH

The HBT-layers were grown on (001) $\pm 0.5^\circ$ oriented s.i. InP:Fe epi-ready substrate in an AIX200-system with rf-heating. The non-gaseous sources are based on TBAs/TBP/TMAs as group-V, DitBuSi/CBr₄ as group-IV n - and p -type dopant sources and the metalorganics TMIn/TEGa/TMAI as group-III precursors. This ngs-configuration increases the safety in LP-MOVPE growth and additionally simplifies the process control due to the decrease the growth temperature and V/III-ratio ramping at the base-emitter heterojunction. For a better doping efficiency of carbon, HBT layer growth is performed using nitrogen (N₂) carrier gas [5,10]. A growth temperature of $T_g = 600 \text{ }^\circ\text{C}$ (V/III = 15) is used for the n -InP emitter layer and $T_g = 620 \text{ }^\circ\text{C}$ (V/III = 5) to grow the n^- , n^+ -InGaAs layers. The p -type InGa(Al)As:C base layers are grown at $T_g = 500 \text{ }^\circ\text{C}$ and very low V/III-ratios of V/III = 0.7 while the doping activation is done by in-situ thermal annealing at $T_a = 620 \text{ }^\circ\text{C}$ in TMAs/N₂ ambient during cooling down. The maximum achieved hole concentrations at $T_g = 500 \text{ }^\circ\text{C}$ for the p^+ -InGaAlAs:C base layer is $3.8 \cdot 10^{19} \text{ cm}^{-3}$ ($\mu_p = 37 \text{ cm}^2/\text{Vs}$ at 300K, sheet resistance = 730 Ω/\square) and $n^+ = 1 \cdot 10^{19} \text{ cm}^{-3}$ for emitter/collector contact layers at $T_g = 620 \text{ }^\circ\text{C}$, respectively. Details of growth are given in [11,12].

The In -composition in p^+ -InGaAlAs layer is linearly graded from 60% at the base-collector side to 53% at the base-emitter side. This base-grading results in compressive strain at the collector side. The band-diagram

of HBT layer stacks with/without *In*-compositional grading is calculated using SimWindows 1.5.0 [13] at thermal equilibrium neglecting the associated dopant grading (Fig.1). Under these conditions a band-bending of 38 meV is calculated which results for 70 nm base layer to an electric field of 5.4 kV/cm. The *In*-grading with a low *In*-content at the emitter side results in both a compositional and a dopant grading in the intended direction. This way, both effects imply an intrinsic electric field pushing minority electrons to the collector and increasing current gain and transit frequency substantially. Using HR-XRD and photoluminescence measurement we have estimated an *Al*-content of about 6% in InGaAlAs base layer and the band-gap energy is about 0.815 eV at room temperature. Therefore the emitter (InP, $E_g \sim 1.35$ eV) – base (InGaAlAs, $E_g \sim 0.815$) junction has a smaller energy difference of about 0.54 eV rather than 0.6 eV of the conventional InGaAs ($E_g \sim 0.75$ eV) base HBT. Owing to the simulation we have calculated the conduction band discontinuity (ΔE_c) and valence band discontinuity (ΔE_v) of 0.225 eV and 0.315 eV, respectively at the emitter-base junction. The base-collector junction also builds a heterojunction and the energy difference is about 0.065 eV without consideration of the bandgap grading. The complete layer stack is summarized in Table 1.

DEVICE FABRICATION AND RESULTS

Device fabrication is performed using conventional optical lithography and wet chemical selective etching. The active region is oriented parallel to the [010] crystal directions which offer sufficient underetching for self-alignment between emitter and base. Non-alloyed Pt/Ti/Pt/Au metal system is evaporated for all contact layers. For the air-bridge connection between active region and contact pads, Ti/Au is evaporated. Triple mesa topology is realized using $H_3PO_4:H_2O_2:H_2O$ solution for InGaAs layers (emitter-cap, base, collector and subcollector) and concentrated HCl for InP (emitter, buffer), respectively (c.f. Fig. 2).

To characterize the InGaAlAs base HBT (sample M1983) we have compared it with InGaAs base HBT (M1977). Both samples have nominal identical layer stacks with same grading condition and growth parameters excepting the *Al*-content of the sample M1983. The measured electrical data of both samples are summarized in table 2. The given doping levels are measured after HBT-fabrication by Van der Pauw Hall measurements and the sheet-/contact resistances are deduced from TLM-measurements at the base layer. A strong decrease in sheet resistance is obtained due to the higher doping level for the sample M1983 but only a slight decrease in contact resistance is achieved which is attributed to the increasing band-gap for the *p*-InGaAlAs:*C* base layer. The reduction of dc-current gain from 230 to 35 is attributed to the higher doping level and the increasing alloy scattering in the quaternary base layer. Additionally the valence band discontinuity is reduced by adding *Al* from about $\Delta E_v \sim 0.348$ eV (InGaAs-base, M1977) to $\Delta E_v \sim 0.315$ eV (InGaAlAs-base, M1983). Although the value of 35 is still much higher than in other works [e.g. 14], this current gain drop is stronger than our expectation. It is therefore necessary to investigate the characteristics of the *Al*-content quaternary material in more detail.

Figure 3 shows the common emitter output characteristics of both samples. Note that the base current for each sample is different. As expected the offset voltage of the sample M1983 is a little bit smaller than M1977 due to the smaller band-gap difference of the e-b and b-c diodes (about 60 meV). The measured gummel plots also show the smaller turn-on voltage of the sample M1983 in the low V_{BE} regime. Another fact in addition is the output conductance of the sample M1983 is very low resulting in a high Early voltage. The measured breakdown voltage of the sample M1983 at $I_C = 100 \mu A$ ($I_B = 0$) is 6.3 V and much higher than 3.8 V of the sample M1977.

First on-wafer S-parameter measurements were performed using an HP8510C network analyzer in the frequency range from 45 MHz to 40 GHz. The non-deembedded cutoff frequency (f_T) of 117 GHz and maximum oscillation frequency (f_{max}) of 90 GHz are extrapolated (slope of 20 dB/decade) at V_{CE} of 2.0 V and $J_C = 8 \times 10^4$ A/cm² (Fig. 5).

CONCLUSION

We have demonstrated InP/InGaAlAs/InGaAs HBT device operation based on MOVPE grown layer stacks using novel non-gaseous source configuration which enables a safe and simplified epitaxy processing without restriction of the material quality. Due to the addition of 6% *Al* the active hole concentration in the HBT base layer is increased from about $1.5 \cdot 10^{19}$ to $3.8 \cdot 10^{19}$ cm⁻³. The *In*-grading results in an intrinsic electric field within the base layer providing a high dc current gain of $\beta = 35$ at a high p-type doping level.

The fabricated HBT with InGaAlAs-base exhibits smaller offset voltage, turn-on voltage and higher breakdown voltage than the conventional InGaAs base HBT. An improved dc-performance and promising first high frequency data of $f_T = 117$ GHz and $f_{max} = 90$ GHz (not deembedded) are achieved.

REFERENCES

- [1] C.R. Abernathy, S.J. Pearton, F. Ren, W.S. Hobson, T.R. Fullowan, A. Katz, A.S. Jordan, J. Kovalchick: *Carbon doping of III-V compounds grown by MOMBE*, J. Crystal Growth 105 (1990) p. 375
- [2] J. L. Benchimol, J. Mba, B. Sermage, M. Riet, S. Blayac, P. Berdager, A.M. Duchenois, P. Andre, J. Thuret, C. Gonzalez, A. Konczykowska: *Investigation of carbon-doped base materials grown by CBE for Al-free InP HBTs*, J. Crystal Growth 209 (2000) pp. 476-480
- [3] W.S. Hobson, S.J. Pearton, A.S. Jordan: *Redistribution of Zn in GaAs-AlGaAs heterojunction bipolar transistor structures*, Appl. Phys. Lett., vol.56 (1990), p.1251
- [4] M.B. Panish, R.A. Hamm, D. Ritter, H.S. Luftman, C.M. Cotell: *Redistribution of beryllium in InP and GaInAs grown by hydride source molecular beam epitaxy and metalorganic molecular beam epitaxy*, J. Crystal Growth, 112 (1991), pp.343-53.
- [5] D. Keiper, R. Westphalen, G. Landgren: *Comparison of carbon-doping of InGaAs and GaAs by CBr₄ using hydrogen or nitrogen as carrier-gas in LP-MOVPE*, J. Crystal Growth 197 (1999) pp. 25-30
- [6] D. Keiper, P. Velling, W. Prost, M. Agethen, F.J. Tegude, G. Landgren: *MOVPE Growth of InP-based HBT with Carbon Doped InGaAs Base Using TBA, TBP in N₂ Ambient*, accepted for Jpn. J. Appl. Phys.
- [7] J. M. Schneider, K. Bitzer, J. Rieger, H. Heinecke: *Highly carbon-doped GaInAs contact layers grown by using CBr₄ in MBE on MOVPE 1.55 μm GaInAsP/InP MQW laser structures*, J. Crystal Growth 188 (1998) pp. 56-62
- [8] W. C. Liu, H.J. Pan, S.Y. Cheng, W.C. Wang, J.Y. Chen, S.C. Feng, K.H. Yu: *Applications of an InGaAlAs/InP continuous-conduction-band structure for ultralow current operation transistors*, Appl. Phys. Lett. 75 (1999) pp. 572-574
- [9] K. Kurishima, H. Nakajima, S. Yamahata, T. Kobayashi, Y. Matsuo: *Effects of a Compositionally-Graded InGaAs Base in Abrupt-Emitter InP/InGaAs HBTs*, Jpn. J. Appl. Phys., Vol. 34 (1995) pp.1221-1227
- [10] H. Hardtdegen, C. Ungermanns, K. Wirtz, D. Guggi, J. Herion, H. Siekmann, H. Lüth: *Heavy carbon doping in low-pressure metalorganic vapor phase epitaxy of GaAs using trimethylarsenic - a comparison between the carrier gases N₂ and H₂*, J. Crystal Growth 145, pp. 440-446, 1994
- [11] P. Velling, M. Agethen, W. Prost, W. Stolz, F.-J. Tegude: *A comparative study of GaAs- and InP-based HBT growth by means of LP-MOVPE using conventional and non gaseous sources*, accepted for Progress in Crystal Growth and Characterization of Materials (invited),
- [12] P. Velling, M. Agethen, W. Prost, F.-J. Tegude: *InAlAs/InGaAs/InP heterostructures for RTD and HBT device applications grown by LP-MOVPE using non-gaseous sources*, accepted for J. Crystal Growth
- [13] SimWindows, *free software* (<http://www-ocs.colorado.edu/SimWindows/simwin.html>)
- [14] K. Kurishima, S. Yamahata, H. Nakajima, H. Ito, Y. Ishii: *Performance and Stability of MOVPE-Grown Carbon-Doped InP/InGaAs HBT's Dehydrogenated by an Anneal after Emitter Mesa Formation*, Jpn. J. Appl. Phys. Vol. 37 (1998) pp. 1353-1358

Table 1: Epitaxial layer stack of the fabricated HBT grown by LP-MOVPE using ngs-configuration

n^+ -InGaAs (emitter cap)	$1 \times 10^{19} \text{ cm}^{-3}$	135 nm
n -InP (emitter)	$5 \times 10^{17} \text{ cm}^{-3}$	65 nm
p^+ -In _{0.53} Ga _{0.41} (Al _{0.06})As (base:In-graded)	$3.8 \times 10^{19} \text{ cm}^{-3}$	70 nm
i -InGaAs (collector)	<i>nid.</i>	270 nm
n^+ -InGaAs (sub-collector)	$1 \times 10^{19} \text{ cm}^{-3}$	270 nm
i -InP (buffer)	<i>nid.</i>	46 nm
Substrate	s.i. InP (Fe)	

Table 2: The comparison of the electrical data of InGaAlAs base HBT with InP/InGaAs HBT

Sample (base layer)	N_A (cm^{-3})	R_{sheet} (Ω/\square)	ρ_c (Ωcm^2)	$V_{\text{CE,offset}}$ (mV)	β_{max}	n_B	n_C	BV_{CEO} @ $I_C = 100 \mu\text{A}$
M1977 ($\text{In}_x\text{Ga}_{1-x}\text{As}$: $x = 0.53 - 0.60$)	$1.5 \cdot 10^{19}$	1700	8 E-6	200	230	1.73	1.25	3.8 V
M1983 ($\text{In}_x\text{Ga}_{1-x}\text{Al}_{0.06}\text{As}$: $x = 0.53 - 0.60$)	$3.8 \cdot 10^{19}$	730	6 E-6	150	35	1.57	1.37	6.3 V

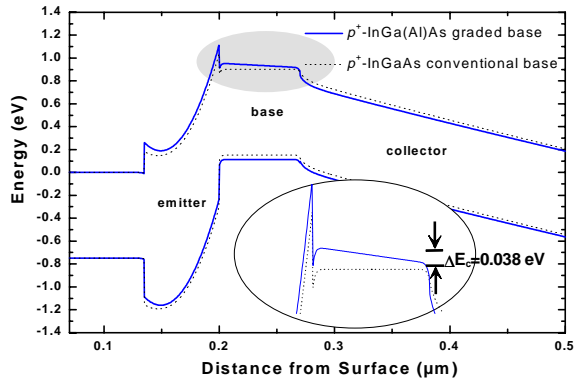


Fig. 1: Calculated energy band diagram of the graded p^+ -InGaAlAs base HBT (solid line) in comparison with the conventional InGaAs base HBT (dotted line) at thermal equilibrium.

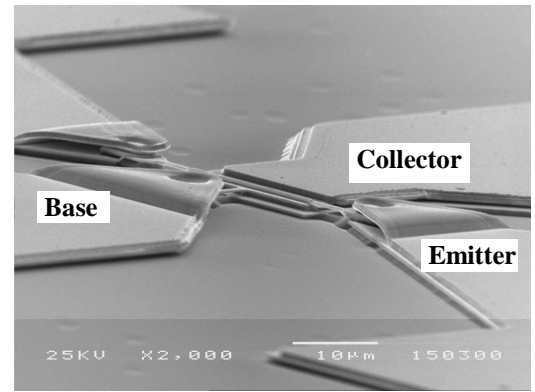


Fig. 2: SEM picture of the fabricated InP/InGaAlAs HBT using conventional optical lithography with wet chemical etching ($A_E = 1 \times 20 \mu\text{m}^2$).

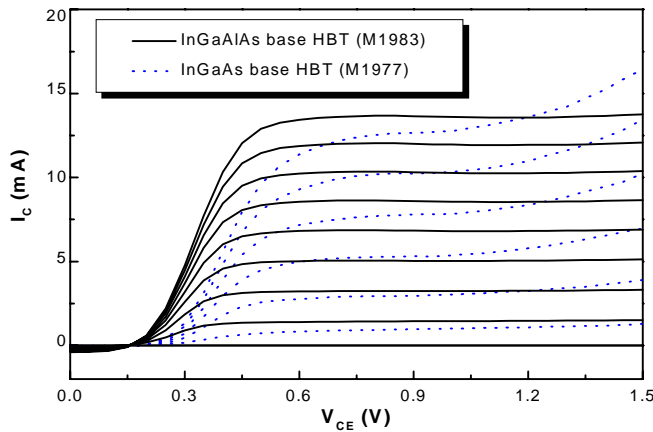


Fig. 3: The common emitter output characteristics of the fabricated HBT with compositionally graded InGaAlAs and InGaAs base layer. Note that the base currents for each sample are different. ($I_{B, \text{InGaAlAs HBT}} = 50 \mu\text{A/step}$, $I_{B, \text{InGaAs HBT}} = 10 \mu\text{A/step}$)

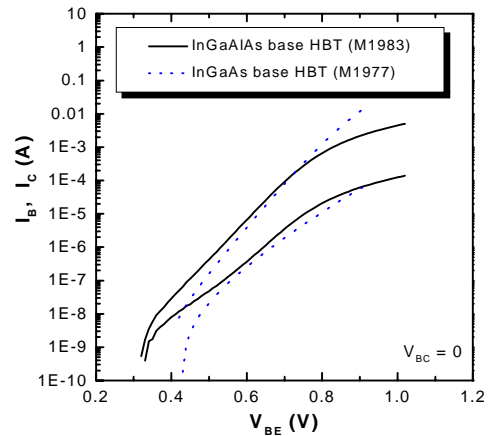


Fig. 4: The Gummel plots of the fabricated InP/InGa(Al)As HBT ($V_{BC} = 0$). See table 2 for ideality factors.

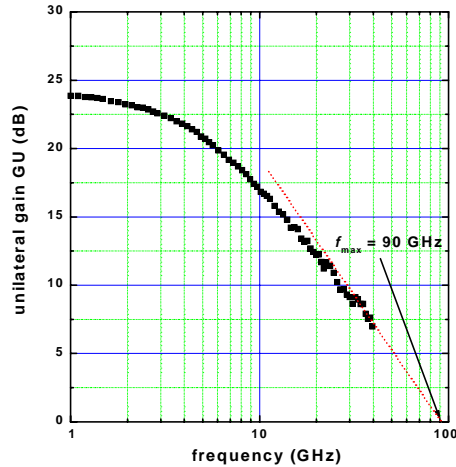
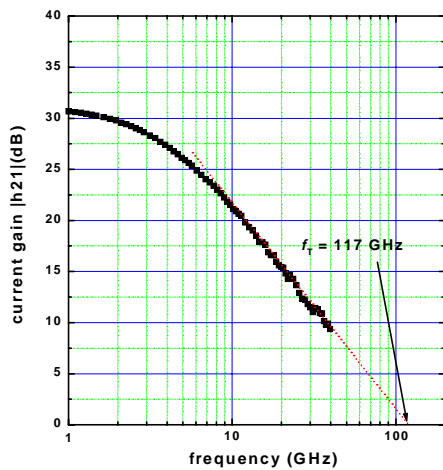


Fig. 5: The measured gain of the fabricated self-aligned InP/InGaAlAs/InGaAs HBT ($A_E = 20 \mu\text{m}^2$). The extrapolated extrinsic f_T and f_{max} are 117 GHz and 90 GHz, respectively.